

On the iron oxide neutral cluster distribution in the gas phase. I. Detection through 193 nm multiphoton ionization

D. N. Shin, Y. Matsuda, and E. R. Bernstein

Citation: *The Journal of Chemical Physics* **120**, 4150 (2004); doi: 10.1063/1.1643732

View online: <http://dx.doi.org/10.1063/1.1643732>

View Table of Contents: <http://aip.scitation.org/toc/jcp/120/9>

Published by the *American Institute of Physics*

COMPLETELY

REDESIGNED!



**PHYSICS
TODAY**

Physics Today Buyer's Guide
Search with a purpose.

On the iron oxide neutral cluster distribution in the gas phase.

I. Detection through 193 nm multiphoton ionization

D. N. Shin, Y. Matsuda, and E. R. Bernstein

Department of Chemistry, Colorado State University, Fort Collins, Colorado 80523-1872

(Received 13 June 2003; accepted 2 December 2003)

Iron oxide (Fe_mO_n) neutral clusters are generated in the gas phase through laser ablation of the metal and reaction with various concentrations of O_2 in He. The mixture of expansion gas and neutral Fe_mO_n cluster species is expanded through a supersonic nozzle into a vacuum system, in which the clusters are ionized by an ArF excimer laser at 193 nm, and the ions are detected and identified in a time-of-flight mass spectrometer. In this report, the experimental parameters that influence the observed cluster distributions, such as ablation laser power, expansion pressure, vacuum system pressure, and 193 nm ArF ionization laser power, are explored. In the second paper in this series, the effect of the ionization laser wavelength (355 nm, 193 nm, 118 nm) on the observed cluster ion distribution is explored. The cluster ion distribution observed employing 193 nm laser ionization, is sensitive to the neutral cluster distribution as evidenced by the change in the observed time-of-flight mass spectra with changes in laser power, growth conditions, and expansion conditions. The thermodynamically stable neutral clusters for saturated O_2 growth conditions are suggested to be of the forms Fe_mO_m , $\text{Fe}_m\text{O}_{m+1}$, and $\text{Fe}_m\text{O}_{m+2}$; which one of these series of neutral clusters is most stable depends on the size of the cluster. For $m < 10$, Fe_mO_m is the most stable neutral cluster series, for $10 \leq m \leq 20$, $\text{Fe}_m\text{O}_{m+1}$ is the most stable neutral cluster series, and for $21 \leq m \leq 30$, $\text{Fe}_m\text{O}_{m+2}$ is the most stable neutral cluster series. Some neutral cluster fragmentation is clearly present for 193 nm ionization due to multiphoton absorption in both the neutral and ionic cluster species. © 2004 American Institute of Physics.
[DOI: 10.1063/1.1643732]

I. INTRODUCTION

The reaction of iron with oxygen to generate iron oxides, especially in the form of small clusters and nanoparticles, is an essential component of a number of fundamental processes, such as environmental corrosion, catalytic behavior and properties, and oxygen transport in biological and other systems. Cluster formation and growth can also offer insight into the transition from molecular behavior to condensed phase behavior, especially for chemical reactivity and catalysis.¹

A number of papers have appeared concerning the formation of iron oxide clusters. We will briefly review them here for general information. Rohlfiing *et al.*² have studied the ionization energies for Fe_m with particular regard to the relationship between ionization energies and chemical reactivity. They also explored the magnetic behavior of Fe_m and $\text{Fe}_m\text{O}_{1,2}$ and found that the magnetic moment of these clusters increases linearly with cluster size. Riley *et al.*³ investigated the chemical reactivity of Fe_m with O_2 in a flow tube reactor system after the iron clusters are formed and cooled. Note that this procedure is quite different from the one we employ to generate Fe_mO_n clusters; nonetheless, their results yield the most stable cluster ions as Fe_mO_m^+ , $\text{Fe}_m\text{O}_{m+1}^+$, $\text{Fe}_m\text{O}_{m+2}^+$ independent of ionization laser wavelength (308, 248, 193 nm). They suggest that up to nine photons of 193 nm radiation can be absorbed by the clusters and that cluster fragmentation during and after the ionization process can be severe. Griffin and Armentrout⁴ studied the kinetic energy

dependence of the reactions of Fe_n^+ ($n=1, \dots, 18$) with CO_2 and O_2 and reported bond energies for Fe_n-O^+ . Wang *et al.*⁵ studied anion photoelectron spectroscopy of iron oxide molecules with up to four Fe and six O atoms. They suggest that each O atom locates on the surface of the Fe_m cluster for $m=3$ and 4. Cluster structures and electronic states are predicted in their studies. Sakurai *et al.*⁶ suggest a trend for stable iron oxide clusters of the form $\text{Fe}_m\text{O}_{(m+3)/2}$ ($m=3, 5, 7, \dots$; that is, Fe_3O_3 , Fe_5O_4 , $\text{Fe}_7\text{O}_5, \dots$) for oxygen deficient clusters of iron oxide. They also stress that Fe_{13}O_8 has a pronounced peak intensity in their oxide ion cluster distribution. Their cluster generation method is different from that of the other workers in this area and also different from that used in our work.

The original motivation for the present study was to obtain baseline data for the investigation of chemical reactions of neutral iron oxide clusters with NO and CO gas phase molecules, with the goal of exploring the Fe_mO_n catalytic activity for the overall reaction $2\text{CO} + 2\text{NO} \rightarrow 2\text{CO}_2 + \text{N}_2$. In this report, we present results on the distribution of iron oxide clusters as determined through multiphoton laser ionization of the clusters at 193 nm and time-of-flight mass spectroscopy (TOFMS). Cluster fragmentation during and following the neutral cluster ionization processes presents a fundamental problem for the determination of the original (prior to reaction or ionization) neutral cluster distribution within the Fe_mO_n cluster beam. This report focuses on the determination of this distribution and how it is influenced by

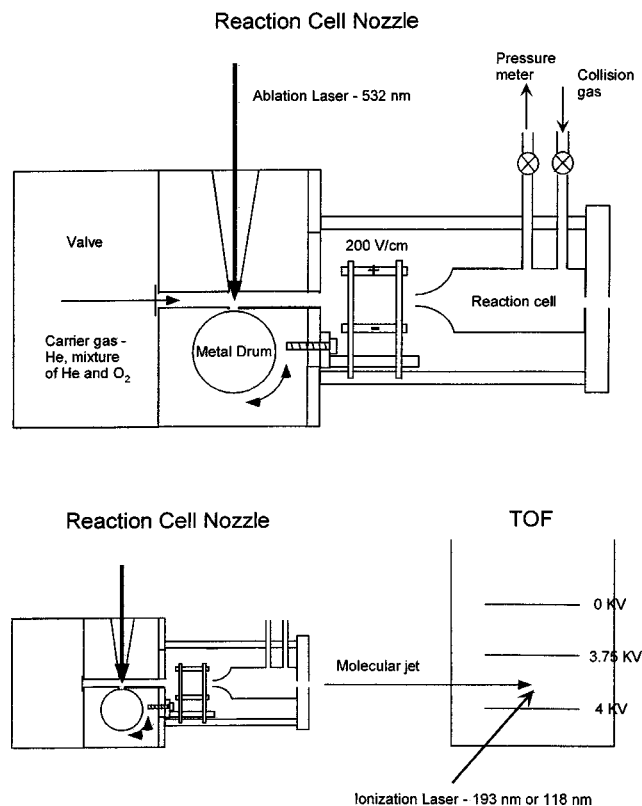


FIG. 1. Schematic drawing of the laser ablation nozzle, electric field ion deflector, reaction cell, and TOFMS ionization region. This apparatus is enclosed in a vacuum chamber with two 6 in. diffusion pumps evacuating the chamber and flight tube. The electric field deflection and reaction cell are not used in these experiments.

193 nm ionization laser power, concentration of oxygen present in the reaction mixture, and other experimental parameters. In a following paper, we discuss the detected cluster distribution as a function of ionization laser wavelength as well. Based on the present study, we suggest the thermodynamically stable neutral clusters, estimate the extent of fragmentation, and compare the results of our studies with those reported previously.²⁻⁶

II. EXPERIMENTAL PROCEDURES

The experimental apparatus and procedures are similar to those used previously by our laboratory.⁷ The nozzle design and overall experimental configuration is represented in Fig. 1. The deflection plates and reaction cell depicted in this schematic are not used in these experiments. The ablation nozzle is based on the now-familiar Smalley design^{7,8} with an R. M. Jordan supersonic pulsed nozzle to which an ablation structure has been attached. The ablation laser (532 nm@10 Hz, doubled Nd/YAG output) energy/pulse is typically less than 5 mJ and is focused to $\approx 100 \mu\text{m}$ on the surface of a rotating drum to which is glued an iron foil (Aldrich, 99.9+%). The drum in this instance can also be machined from iron. The same nozzle system can be employed with a powdered metal oxide sample that can be lightly pressed or glued (crazy glue, sugar water,...) on to the cylindrical drum for laser ablation. The ablation laser creates a plume of iron vapor (Fe , Fe^+ , Fe^- , Fe_m , Fe_m^+ , Fe_m^-),

which evolves into a gas pulse from the nozzle. The composition of the expansion gas will be shown (*vide infra*) to be a major controlling factor in the determination of the neutral cluster distribution. Following the reaction of Fe_m species with O_2 , the iron oxide clusters are entrained in the gas pulse and expanded through the gas channel (2 mm \times 25 mm) into the vacuum chamber held at $\sim 5 \times 10^{-6}$ Torr during the ablation process. The neutral clusters pass into the mass spectrometer, they are ionized by the ionization laser pulse (in this instance, an ArF excimer laser, 193 nm <2 mJ/pulse@10 Hz), and extracted into the flight tube perpendicular to their flow direction by a 4.0 kV electric field. The TOFMS is of a Wiley-McLaren design.⁷

Ions are detected at the end of a 1.5 m flight tube by a dual microchannel plate detector. The output of this detector is digitized by a Techtronix digitizing recorder (RTD 720A) at a rate of up to 2 G samples/s. Typically 2000 spectra are individually collected and individually stored for further analysis.⁷ Averaged data or individual spectra can be generated and compared in this approach.

Note that the observed and presented spectra in this report, and in the following report,⁹ are often a sensitive function of the experimental parameters, such as timing of lasers and valve opening, laser power, laser focal size, and TOFMS settings. Thus, for essentially the “same experimental conditions,” one can, to some extent, vary the relative intensities of different series of clusters (e.g., $\text{Fe}_m\text{O}_{m\pm 1, \pm 2}$, etc.). These differences are small and do not affect the general conclusions one can draw from the overall experimental findings.

III. RESULTS

Figure 2 shows the TOF mass spectra taken at four different O_2 concentrations in the He expansion gas: (a) 2%; (b) 1%; (c) 0.5%; and (d) 0.1% in 20 psig He carrier gas. In these spectra, ablation and ionization laser powers are 35 and 11.5 mW, respectively. As shown in Figs. 2(a), 2(b), 2(c), the mass spectra reveal a series of iron oxide clusters of the form Fe_mO_n^+ ($m \leq n$). Under these experimental conditions, no Fe_m clusters are observed, and the major cluster series are Fe_mO_m^+ and $\text{Fe}_m\text{O}_{m+1}^+$. Decreasing the O_2 concentration from 2% to 0.5% has the effect of increasing the intensity of the TOFMS cluster spectra and stabilizing the overall distribution. At 0.1% O_2 concentration, oxygen deficient clusters begin to appear as $\text{Fe}_m\text{O}_{m-1}^+$ [Fig. 1(d)] and the overall Fe_mO_n cluster distribution becomes narrower. Note that the prominent features in these cluster spectra are still of the form Fe_mO_m^+ and $\text{Fe}_m\text{O}_{m+1}^+$, and that, at low concentration of O_2 , appearance of $\text{Fe}_m\text{O}_{m-1}^+$ in the mass spectrum is probably a kinetic result and not a thermodynamic one.

Under these experimental conditions and nozzle design and structure, the most intense and stable Fe_mO_n^+ mass spectra are obtained at 0.75% O_2/He as shown in Fig. 3. The series of clusters for this condition are Fe_mO_m^+ , $\text{Fe}_m\text{O}_{m+1}^+$, and $\text{Fe}_m\text{O}_{m+2}^+$. The more oxygen rich clusters appear for larger cluster sizes ($m > 6$ for $\text{Fe}_m\text{O}_{m+1}^+$ and $m > 12$ for $\text{Fe}_m\text{O}_{m+2}^+$).

Oxygen deficient clusters (Fe_mO_n , $m > n$) might be more reactive than oxygen rich clusters, while oxygen rich clusters

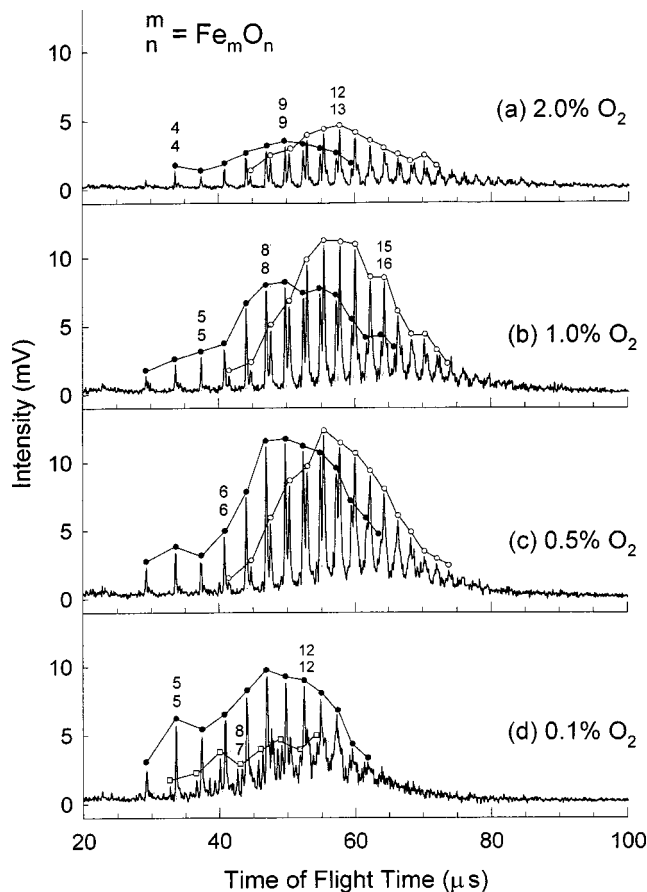


FIG. 2. TOF mass spectra of iron oxide clusters taken at four different oxygen concentrations: (a) 2.0%; (b) 1.0%; (c) 0.5%; and (d) 0.1% in 20 psig He carrier gas, 35 mW ablation, and 11.5 mW ionization laser powers. Each peak is classified by symbols according to the number of Fe and O atoms: closed circle, Fe_mO_m^+ ; open circle, $\text{Fe}_m\text{O}_{m+1}^+$.

($\text{Fe}_m\text{O}_n, m < n$) might be more catalytically active than oxygen deficient clusters. Thus, adjusting the experimental conditions to favor one set of clusters over the other in the neutral cluster distribution could be useful. As mentioned above,

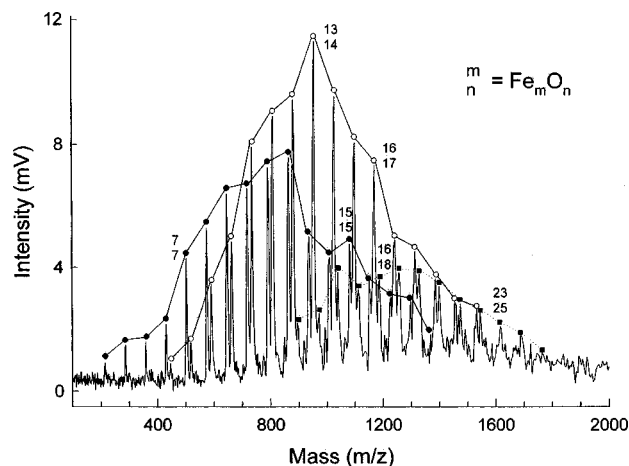


FIG. 3. TOF mass spectrum of iron oxide clusters showing the series of clusters Fe_mO_m^+ , $\text{Fe}_m\text{O}_{m+1}^+$, and $\text{Fe}_m\text{O}_{m+2}^+$ (0.75% O_2 in 20 psig He, ablation laser power of 34 mW, and ionization laser power of 11 mW). Closed circles, open circles, and closed squares show positions of Fe_mO_m^+ , $\text{Fe}_m\text{O}_{m+1}^+$, $\text{Fe}_m\text{O}_{m+2}^+$ clusters, respectively.

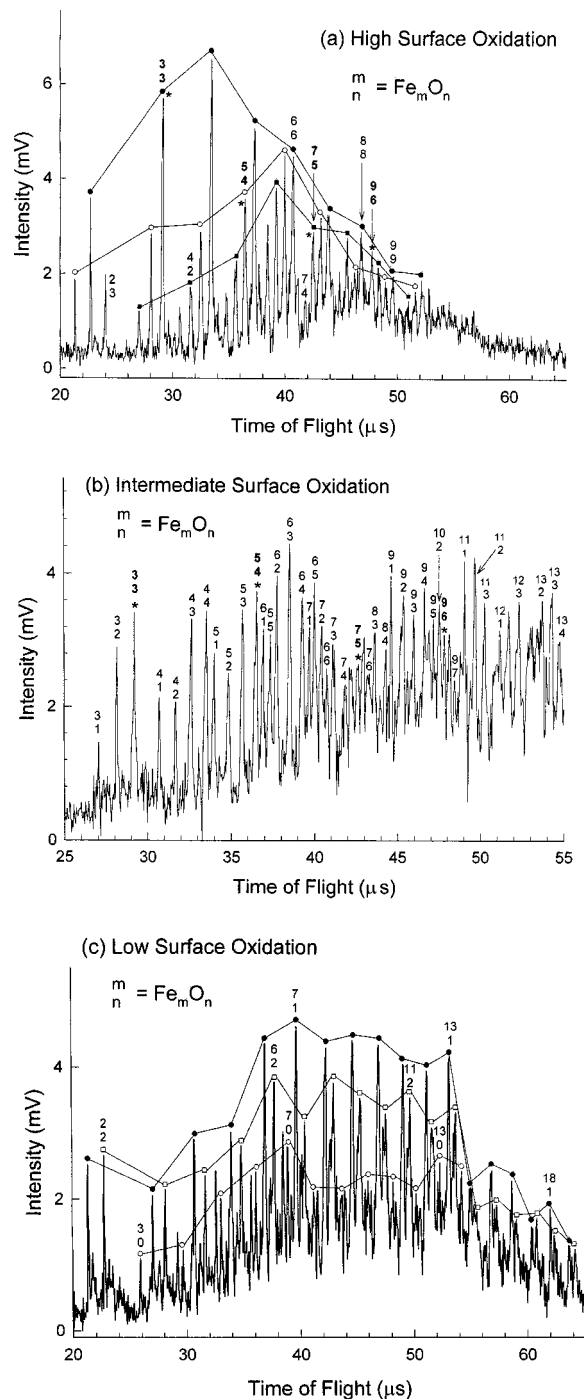


FIG. 4. TOF mass spectra of iron oxide clusters obtained by ablation of three different surface oxidation conditions for an iron surface with no added oxygen in expansion gas (20 psig He and 5 Hz) (a) high oxidation. Closed circles, open circles, and closed squares show positions of Fe_mO_m^+ , $\text{Fe}_m\text{O}_{m-1}^+$, $\text{Fe}_m\text{O}_{m-2}^+$ clusters, respectively; (b) intermediate oxidation. Closed circles, open squares, and open circles show positions of Fe_mO_1 , Fe_mO_2 , and Fe_m clusters, respectively; and (c) low oxidation. Note that Fe_{13}O_8 and Fe_{15}O_1 (●) are degenerate in mass in (c) and that the * in (a) and (b) marks clusters of the form $\text{Fe}_m\text{O}_{(m+3)/2}^+$ for $m=3, 5, 7, 9$.

only Fe_mO_n ($n \geq m$) clusters are observed by 193 nm ionization with more than 0.1% O_2 present in the expansion gas. Oxygen deficient clusters can be generated with no O_2 in the expansion gas, but the surface condition of the iron metal is important for the clusters that are observed. In Fig. 4, the

cluster distribution is displayed for surfaces of three different degrees of oxidation. Figure 4(a) shows a fresh, nonablated Fe surface that has been exposed to air for a long time. Figure 4(b) shows the cluster distribution derived from the Fig. 4(a) surface following one laser ablation, and Fig. 4(c) shows the cluster distribution derived from the same surface twice laser ablated. Under our experimental conditions, generation of oxygen deficient or pure metal clusters is quite difficult. This series of mass spectra demonstrates that oxygen rich and poor iron clusters can be observed by 193 nm laser ionization and, in particular, that such ionization does not completely lose information concerning cluster growth and neutral cluster distribution. Timing of events and laser conditions are not changed for these experiments. Even with no oxygen in the expansion, Fe_mO_m^+ are still the prominent features in Fig. 4(a).

After the surface of the iron sample has been ablated once, the second ablation pass generates a set of Fe_mO_n clusters that are significantly more oxygen deficient. In the low mass region, the dominant clusters are still of the form Fe_mO_m with $m=3, 4$, but, as the number of iron atoms in the cluster increases, oxygen deficient clusters begin to dominate the mass spectrum [Fig. 4(b)]. Fe_mO_m^+ for $m=5, 6, 7$, become only a minor species in the mass spectrum and eventually $\text{Fe}_m\text{O}_{1,2,3,4}^+$ clusters dominate the spectrum at $m \geq 8$. With the next pass over the same Fe metal surface, pure Fe_m^+ and $\text{Fe}_m\text{O}_{1,2}^+$ clusters are the main features in the mass spectrum [Fig. 4(c)]. Clearly these spectra display growth kinetics and not thermodynamic stability or predominantly fragmentation. The results demonstrate that the formation of neutral iron oxide clusters in the ablation process is significantly controlled by the oxygen concentration in the plume formed by the ablation. Additionally, Fe_mO_n cluster growth, controlled in large measure by oxygen content in the plasma plume, is a major factor in the observed TOFMS of the Fe_mO_n clusters detected by 193 nm laser ionization.

Figure 5 displays the mass spectra of cluster ions generated at 0.75% O_2/He @ 110 psig as a function of 193 nm ionization laser power. At 20 mW (2 mJ/pulse) focused to $\approx 0.5 \text{ mm} \times 2 \text{ mm}$, with the long dimension of the laser beam collinear with the molecular beam axis, no mass spectral features are observed. Most likely complete cluster fragmentation occurs due to multiphoton absorption and ionization [see Fig. 5(a)]: only the Fe^+ feature is observed. With an ionization laser power of 17 mW [Fig. 5(b)], iron oxide clusters begin to appear in the form Fe_mO_m^+ ($m=2, \dots, 14$) and $\text{Fe}_m\text{O}_{m+1}^+$ ($m=8, \dots, 17, \dots$). Small iron oxide clusters are readily observed at this power up to $\text{Fe}_{16}\text{O}_{17}^+$; however, the larger clusters displayed in Figs. 2 and 3 must still be fragmented at this power. As the ionization laser power is further decreased from 17 to 8 mW, the generation of iron oxide cluster ions is observed with both wide distribution and significant intensity [Figs. 5(c), 5(d), 5(e)]. Further reduction in ionization laser power to 6 mW [Fig. 5(f)] shows lower cluster ion intensity and a broader distribution to higher mass. Note the trend with all of these spectra, but especially for Figs. 5(c), 5(d), 5(e), 5(f), that small iron oxide cluster ions Fe_mO_m^+ ($m \leq 7$) are not observed as the ionization laser power decreases to 6 mW. This observation is discussed in

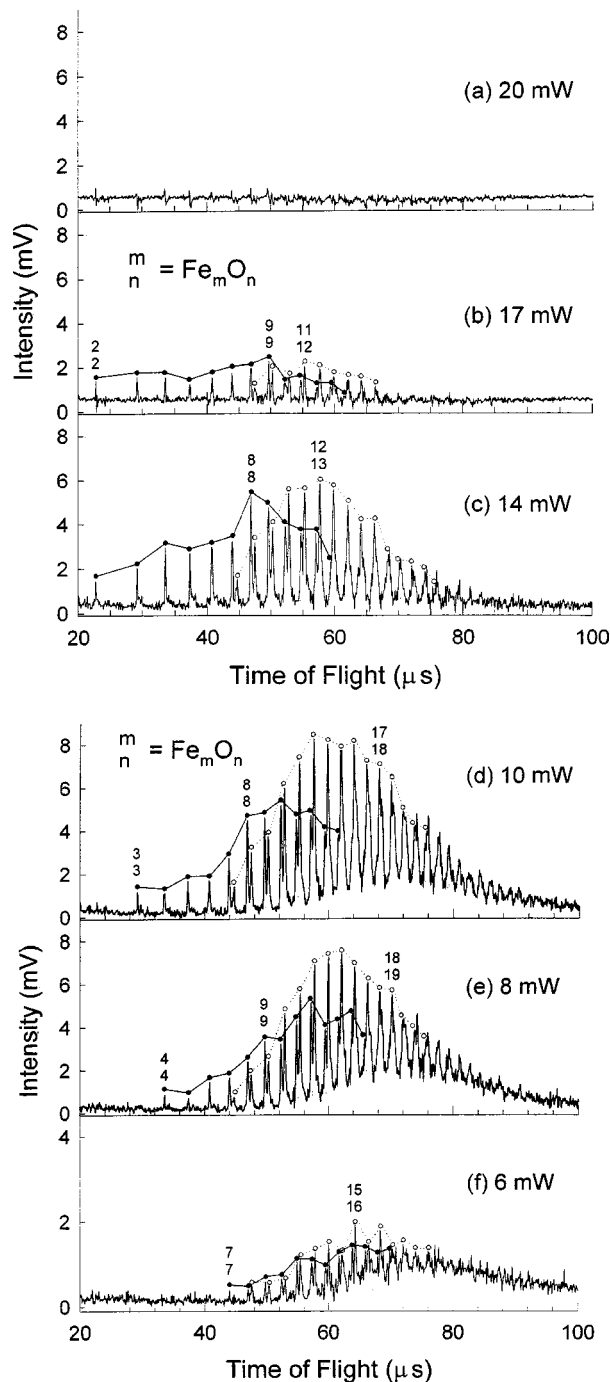


FIG. 5. TOF mass spectra as a function of ionization laser power (0.75% O_2 in 110 psig He, and ablation laser power of 25 mW). Closed and open circles show positions of Fe_mO_m^+ and $\text{Fe}_m\text{O}_{m+1}^+$ clusters.

the next section with respect to ionization/fragmentation mechanisms and the neutral cluster distribution.

In addition to oxygen concentration and ionization laser power, we also explore the dependence of the TOFMS on ablation laser power, backing pressure, and chamber pressure. In the power range 20–50 mW, the ablation laser power has little influence on the observed cluster ion distribution, but the spectra are most intense for an ablation laser power of 30–40 mW. Variation of the backing pressure by as much as a factor of 6 for the expansion has little effect on the cluster distribution. The Fe_mO_n^+ mass spectral signal can also

be a function of the vacuum chamber pressure. At the lower chamber pressure (3 Hz repetition rate of nozzle), the best mass resolution obtains. Clearly the ions must undergo some collisions as they are extracted from the ionization region for a 10 Hz experiment as the system pumping speed is fixed for all experiments.

IV. DISCUSSION

The main goal of these studies is to evaluate the neutral iron oxide cluster distribution for a given set of cluster growth conditions. Eventually, one would want to control this distribution, to the extent possible, to include or emphasize, for example, oxygen deficient $\text{Fe}_m\text{O}_{m-x}$, oxygen rich $\text{Fe}_m\text{O}_{m+x}$ ($1 \leq x \leq 3$), one-to-one Fe_mO_m , mostly metallic $\text{Fe}_m\text{O}_{1,2}$, large Fe_mO_n ($m > 10$), or small Fe_mO_n ($m < 10$) clusters. The Results presents data that would suggest such fine tuning of the neutral cluster distribution is certainly a possibility.

In this discussion of the results, we will analyze the data of the last section to extract information concerning the neutral cluster distribution of Fe_mO_n and compare the results of the present studies with those found in the literature. We focus on the two experimental parameters that appear to have the most influence on the observed mass spectrum of iron oxide cluster ions: oxygen content of the sample and the expansion gas, and ionization laser power.

A. Oxygen concentration and 193 nm ionization laser power dependence of the detected cluster ions

The data presented in Figs. 2–4 make clear that the neutral iron oxide cluster distribution is readily influenced and controlled by the concentration of oxygen in the expansion gas and the oxygen content of the ablated iron metal surface. If an excess of oxygen is present for the reaction system, a set of cluster ions is observed of the form Fe_mO_m^+ and $\text{Fe}_m\text{O}_{m+1,2}^+$ ($m \leq 25$). If the oxygen content of the system is reduced, a variety of Fe_mO_n^+ ($m > n$) begins to appear. These oxygen deficient clusters must be kinetically controlled because if sufficient oxygen is present, they grow to one-to-one or oxygen rich species. The ionization process may indeed cause some fragmentation of the neutral clusters, and may in particular influence intensities of the observed features to some extent, but it cannot be responsible for the gross behavior of the distribution as a function of O_2 content in the ablation/expansion system. The observed cluster ion distribution reflects the nature of the neutral cluster distribution and reveals which clusters may be thermodynamically stable and which are kinetically controlled. The neutral cluster distribution may well be richer than revealed by the 193 nm multiphoton ionization processes (especially with respect to clusters that might not appear in the TOFMS), but the observed spectra are clearly growth and neutral distribution controlled.

193 nm (6.4 eV) laser ionization occurs by multiphoton absorption because many of the small clusters, if not all clusters observed, have ionization thresholds above 6.4 eV. Also, these clusters have a high density of vibronic states so that resonant absorption of photons is possible and vibronic relaxation is quite fast. Thus, during a 10 ns laser pulse, many photons can be absorbed by a cluster, and internal relaxation

within the cluster can occur. Both intracluster vibrational relaxation (IVR) and vibration predissociation (VP) of the clusters depend on cluster density of states: IVR rate constants can be approximated by Fermi's Golden rule and VP rate constants can be estimated by RRKM theory.¹⁰ Thus, large clusters have fast IVR ($\tau_{\text{IVR}} \sim 1$ ps) and slow VP ($\tau_{\text{VP}} \sim 1$ μ s) and small clusters have slow IVR ($\tau_{\text{IVR}} \sim 1$ μ s) and fast VP ($\tau_{\text{VP}} \sim 1$ ps), of course depending on density of states, excess energy in the cluster, Franck–Condon factors, etc.¹⁰ At low density of states for small clusters, absorption cross sections can also become small.

The experimental conditions required to generate two photon ionization for the iron oxide clusters can also generate vertical multiphoton absorption of more than two photons. Additionally, the laser light is present for ≈ 10 ns, which is a long time compared to molecular and ion dynamical processes prior to cluster fragmentation. Thus, the clusters may fragment as neutral or as ions during this time and at subsequent times as well. We cannot determine, in these experiments, whether fragmentation occurs for the neutral or the ion.

Figure 5 demonstrates the influence of 193 nm laser ionization power (related to multiphoton/fragmentation processes) on the observed cluster ion intensities in the mass spectrum. Such dependence corroborates the idea that, at this laser wavelength, neutral cluster fragmentation during the ionization process does influence the observed cluster ion distribution. We also know that the effect of 193 nm ionization laser energy/pulse must be a perturbation on the neutral cluster distribution and not the controlling effect based on mass spectra obtained as a function of oxygen concentration and growth conditions (see Figs. 2, 3, 4). In the spectra of Figs. 2, 3, and 4, we see that small clusters are indeed present in the mass spectra as the O_2 content of the sample is varied at fixed ionization energy/pulse. Note, too, that large clusters tend to have lower ionization energies than small ones. Thus, one cannot conclude that the loss of small cluster ions at low laser energy/pulse is due to a reduction in fragmentation of large clusters. The reason for the absence of small clusters at low ionization laser power must be that these clusters have a reduced ionization (multiphoton) cross section due to their lower cluster density of states and higher ionization energies compared to larger clusters. This implies that the observation of Fe_mO_m^+ , $\text{Fe}_m\text{O}_{m+1}^+$, $\text{Fe}_m\text{O}_{m+2}^+$ features in the mass spectra truly reflect the presence of such neutral species in the neutral cluster distribution. One can thereby suggest that these neutral clusters near one-to-one Fe/O ratios are the thermodynamically stable clusters in the presence of excess oxygen. At lower oxygen concentrations in the system, the observed oxygen deficient clusters ($\text{Fe}_m\text{O}, \dots, \text{Fe}_m\text{O}_{m-1,2,3, \dots}$) are present due to restricted reaction/diffusion kinetics as the sample cools.

B. Comparison with previous iron oxide cluster results

With oxygen in the expansion gas and for a high concentration of surface oxygen on iron through exposure to air, the thermodynamically stable neutral Fe_mO_m , $\text{Fe}_m\text{O}_{m+1}$, and $\text{Fe}_m\text{O}_{m+2}$ clusters are present in the beam, as suggested

above. These results are in complete agreement with those of Riley and co-workers³ using a very different reaction scheme from the one presented here. In these previous studies, iron metal clusters are formed, cooled to room temperature, and passed through a flow tube reactor to form Fe_mO_n clusters. In our situation, one can think of the neutral cluster growth mechanism as schematically represented by $m\text{Fe} + n\text{O} \rightarrow \text{Fe}_m\text{O}_n$ in a step-by-step process. A suggested mechanism for the formation of similar clusters from such different reactants ($\text{Fe}_m + x\text{O}_2 \rightarrow \text{Fe}_m\text{O}_n$) is that the ΔH for the reaction of Fe with O is so large that the Fe_m clusters are heated to 10^3 – 10^4 K such that an atomic mechanism applies in both circumstances. Bond energies for $\text{Fe}_n^+ - \text{O}$ and $\text{Fe}_n^+ \text{O}_2$ are 3.8–5.2 and 9–12 eV, respectively.⁴ This would attest to the fact that, in the presence of excess oxygen (both cases), the Fe_mO_m and $\text{Fe}_m\text{O}_{m+1,2}$ clusters are truly the thermodynamically stable neutral clusters for $m \leq 30$, at least.

On the other hand, the oxidized or adsorbed iron surface studies (for which oxygen exists in the system in less than stoichiometric amounts) show that oxygen deficient clusters can be generated (under kinetic/diffusion control) in the beam. Nonetheless, even under these conditions, Fe_mO_m^+ clusters can be found along with Fe_mO_n^+ ($n < m$). This is in accord with the findings of Sakuri and co-workers,⁶ who also apparently employed oxygen deficient conditions in their experiments. Note that their nozzle design is unique and different than the one employed in the present experiments.

Sakuri and co-workers⁶ have found, under oxygen deficient conditions, that the intensity of cluster ions of the form $\text{Fe}_m\text{O}_{(m+3)/2}^+$ ($m = 3, 5, 7, \dots$) is enhanced. We have also found this tendency as can be seen in Fig. 4 for the features designated with an asterisk. For example, from Fig. 4(b) Fe_7O_5^+ is more intense than Fe_7O_4^+ , Fe_3O_3^+ is more intense than Fe_3O_2^+ and Fe_5O_4^+ is more intense than Fe_5O_3^+ : this is not the expected trend for random growth of clusters based on cluster size. Since these features do not appear as special under conditions of excess oxygen in the system, however, we conclude their presence is a result of kinetic growth control and not thermodynamic stability. These workers also suggest the presence of a “special” stable cluster at Fe_{13}O_8 . We note that, under the oxygen starved conditions of Fig. 4(c), we also see an enhanced intensity for $\text{Fe}_{13}\text{O}_8^+$ as has been reported by Sakuri and co-workers.⁶ This feature is degenerate in mass with the series Fe_mO_1^+ for $m = 15$. We do not suggest that $\text{Fe}_{13}\text{O}_8^+$ is of any special intensity, but it may be present due to a kinetic or diffusional process under these specific, but reproducible, experimental conditions.

V. CONCLUSIONS

We have studied the neutral cluster distribution of iron oxide clusters formed by laser ablation of iron metal and reaction of the metal plasma plume with oxygen in the gas phase under a wide variety of experimental conditions including oxygen concentration and 193 nm ionization laser power, among other variables. These two conditions appear to be the most sensitive ones for the determination of the neutral cluster behavior. Under conditions of excess oxygen, clusters that are thermodynamically stable are identified. Un-

der conditions of insufficient oxygen for the growth process, oxygen deficient clusters, whose oxygen content is kinetically controlled, are observed. The nature of the observed neutral iron oxide clusters can thus be controlled through variation of the oxygen content of the ablation/expansion process.

The major conclusions from these studies are given below.

- (1) The most stable clusters observed under conditions of excess oxygen are of the forms Fe_mO_m and $\text{Fe}_m\text{O}_{m+1,2}$. The latter more oxygen rich clusters appear to dominate the distribution at $m \geq 10$.
- (2) Several oxygen deficient cluster series are observed if the oxygen concentration in the system is reduced to only the surface adhered oxygen on the iron metal foil. Under such conditions of cluster growth controlled by diffusion and other kinetic processes, Fe_mO_n ($n = m - 1, m - 2, m - 3$), and finally Fe_m , Fe_mO_n ($n = 1, \dots, 4, m > 7$) cluster series are observed. Even under these oxygen deficient conditions, the most stable Fe_mO_m cluster series is observed to have substantial concentration for $m \leq 6$.
- (3) Under our experimental conditions, special clusters, aside from the thermodynamically controlled and kinetically controlled series mentioned above, are not readily obvious.
- (4) Using a 193 nm ionization laser for detection of the neutral cluster distribution surely causes some fragmentation of the neutral clusters and thus, may affect the relative intensities of some features or cluster series; nonetheless, the major features of the mass spectrum can be analyzed to obtain a good estimate of the neutral cluster distribution underlying the observed cluster ion distribution. This neutral cluster distribution can be thermodynamically or kinetically controlled, depending on the concentration of oxygen in the system.

ACKNOWLEDGMENTS

This research is supported in part by grants from Philip Morris USA and the U.S. Department of Energy.

¹(a) E. L. Muttart, T. N. Rodin, E. Brand, C. F. Brucker, and W. Pretzer, *Chem. Rev.* **79**, 91 (1979); (b) K. Eller and H. Schwarz, *ibid.* **91**, 1121 (1991), and references therein to earlier work; (c) D. Schröder and H. Schwarz, *Angew. Chem., Int. Ed. Engl.* **34**, 1973 (1995); (d) G. Ertl and H. J. Freund, *Phys. Today* **52**, 32 (1999); (e) P. A. Hackett, S. A. Mitchell, D. M. Rayner, and B. Simard, in *Metal-Ligand Interactions*, edited by R. Russo and D. R. Salahub (Kluwer, Amsterdam, 1996), p. 289.

²(a) E. A. Rohlfling, D. M. Cox, and A. Kaldor, *Chem. Phys. Lett.* **99**, 161 (1983); (b) D. M. Cox, D. J. Trevor, R. L. Whetten, E. A. Rohlfling, and A. Kaldor, *Phys. Rev. B* **32**, 7290 (1985); (c) E. A. Rohlfling, D. M. Cox, A. Kaldor, and K. H. Johnson, *J. Chem. Phys.* **81**, 3846 (1984).

³(a) S. J. Riley, in *Metal-Ligand Interactions: From Atoms, to Clusters, to Surfaces*, edited by D. R. Salahub and N. Russo (Kluwer Academic, The Netherlands, 1992), pp. 17–36; (b) G. C. Nieman, E. K. Parks, S. C. Richtsmeier, K. Liu, L. G. Pobo, and S. J. Riley, *High. Temp. Sci.* **22**, 115 (1986).

⁴(a) J. B. Griffin and P. B. Armentrout, *J. Chem. Phys.* **106**, 4448 (1997); (b) **107**, 5345 (1997).

⁵(a) L.-S. Wang, H. Wu, and S. R. Desai, *Phys. Rev. Lett.* **76**, 4853 (1996); (b) H. Wu, S. R. Desai, and L.-S. Wang, *J. Am. Chem. Soc.* **118**, 5296

- (1996); (c) L.-S. Wang, J. Fan, and L. Lou, *Surf. Rev. Lett.* **3**, 695 (1996).
- ⁶(a) M. Sakurai, K. Sumiyama, Q. Sun, and Y. Kawazoe, *J. Phys. Soc. Jpn.* **68**, 3497 (1999); (b) M. Sakurai, K. Watanabe, K. Sumiyama, and K. Suzuki, *ibid.* **67**, 2571 (1998); (c) Q. Wang, Q. Sun, M. Sakurai, J. Z. Yu, B. L. Gu, K. Sumiyama, and Y. Kawazoe, *Phys. Rev. B* **59**, 12672 (1999); (d) Q. Sun, M. Sakurai, Q. Wang, J. Z. Yu, G. H. Wang, K. Sumiyama, and Y. Kawazoe, *ibid.* **62**, 8500 (2000); (e) Q. Wang, Q. Sun, M. Sakurai, J. Z. Yu, B. L. Gu, K. Sumiyama, and Y. Kawazoe, *ibid.* **59**, 12672 (1999); (f) Q. Sun, M. Sakurai, Q. Wang, J. Z. Yu, G. H. Wang, K. Sumiyama, and Y. Kawazoe, *ibid.* **62**, 8500 (2000); (g) M. Sakurai, K. Watanabe, K. Sumiyama, and K. Suzuki, *J. Chem. Phys.* **111**, 235 (1999).
- ⁷(a) M. Foltin, G. J. Stueber, and E. R. Bernstein, *J. Chem. Phys.* **109**, 4342 (1998); (b) **111**, 9577 (1999); (c) **114**, 8971 (2001).
- ⁸R. E. Smalley, in *Atomic and Molecular Clusters*, edited by E. R. Bernstein (Elsevier, New York, 1990), p. 1.
- ⁹D. N. Shin, Y. Matsuda, and E. R. Bernstein, *J. Chem. Phys.* **120**, 4157 (2004), following paper.
- ¹⁰(a) D. F. Kelley and E. R. Bernstein, *J. Phys. Chem.* **90**, 5164 (1986); (b) M. R. Nimlos, M. A. Young, E. R. Bernstein, and D. F. Kelley, *J. Chem. Phys.* **91**, 5268 (1989); (c) M. F. Hineman, S. K. Kim, E. R. Bernstein, and D. F. Kelley, *ibid.* **96**, 4904 (1992); (d) M. Hineman, D. F. Kelley, and E. R. Bernstein, *ibid.* **99**, 4533 (1993); (e) M. Hineman, E. R. Bernstein, and D. F. Kelley, *ibid.* **98**, 2516 (1993); (f) M. Hineman, E. R. Bernstein, and D. F. Kelley, *ibid.* **101**, 850 (1994); (g) E. R. Bernstein, *Annu. Rev. Phys. Chem.* **46**, 197 (1995).